

# The Structure of Oleamide Films at the Aluminum/Oil Interface and Aluminum/Air Interface Studied by Sum Frequency Generation (SFG) Vibrational Spectroscopy and Reflection Absorption Infrared Spectroscopy (RAIRS)

Michael T. L. Casford\* and Paul B. Davies

Department of Chemistry, University of Cambridge, Lensfield Road, Cambridge CB2 1EW, United Kingdom

**ABSTRACT** The structure of oleamide (*cis*-9-octadecenamide) films on aluminum has been investigated by sum frequency generation vibrational spectroscopy (SFG) and reflection absorption infrared spectroscopy (RAIRS). Three different film deposition strategies were investigated: (i) films formed by equilibrium adsorption from oleamide solutions in oil, (ii) Langmuir–Blodgett films cast at 1 and 25 mN m<sup>-1</sup>, (iii) thick spin-cast films. Both L–B and spin-cast films were examined in air and under oil. The adsorbate formed in the 1 mN m<sup>-1</sup> film in air showed little orientational order. For this film, the spectroscopic results and the ellipsometric thickness point to a relatively conformationally disordered monolayer that is oriented principally in the plane of the interface. Direct adsorption to the metal interface from oil results in SFG spectra of oleamide that are comparable to those observed for the 1 mN m<sup>-1</sup> L–B film in air. In contrast, SFG and RAIRS results for the 25 mN m<sup>-1</sup> film in air and SFG spectra of the spin-cast film in air both show strong conformational ordering and orientational alignment normal to the interface. The 25 mN m<sup>-1</sup> film has an ellipsometric thickness almost twice that of the 1 mN m<sup>-1</sup> L–B film. Taken in combination with the spectroscopic results, this is indicative of a well packed monolayer in air in which the hydrocarbon chain is in an essentially defect-free extended conformation with the methyl terminus oriented away from the surface. A similar structure is also deduced for the surface of the spin-cast film in air. Upon immersion of the 25 mN m<sup>-1</sup> L–B film in oil the SFG spectra show that this film rapidly adopts a relatively disordered structure similar to that seen for the 1 mN m<sup>-1</sup> L–B film in air. Immersion of the spin-cast film in oil results in the gradual disordering of the amide film over a period of several days until the observed spectra become essentially identical to those observed for direct adsorption of oleamide from oil.

**KEYWORDS:** aluminium • oil • oleamide • adsorption • sum frequency spectroscopy

## INTRODUCTION

Oleamide has received considerable attention in recent years as a biologically and neurologically active lipid (1–4). However, relatively little attention has been paid to its function as a slip additive for polymeric (5, 6) and metallic friction modification (7, 8), despite the generic use of amides as antiwear additives reported in the literature (9–11). The use of commercial grade oleamide is well-established in both the polymer industry and in metal fabrication, where it is used to prevent the adhesion of polymer films, and in the drawing of metal wire and the extrusion of aluminum sections. Little work has been done from a fundamental perspective, however, concerning the structure that oleamide adopts upon adsorption to surfaces in general (12–14) and to metal surfaces such as aluminum in particular. To date, the majority of published work has focused mainly on dried films cast from volatile

organic solvents such as methanol or chloroform. Among the adsorption studies reported, that of Miyashita et al. (13) and of Zhang et al. (14) focused on the specific interactions between an oleamide film and a graphite lattice, in which the van der Waals interactions between the aliphatic chain and the carbon lattice dominate the adsorption characteristics leading to a crystalline ordering in the plane of the interface. In contrast, Yijun Gu et al. (12), utilizing both spin-cast and multilayer Langmuir–Blodgett (L–B) films on silver, suggested a perpendicular orientation of the aliphatic chain with the amide carbonyl group orienting in the plane of the interface. These adsorption structures represent two extremes in respect of the polar orientation of the adsorbed film and give little indication as to the structure likely to be adopted by oleamide when adsorbing to a metallic surface from a low concentration in lubricating oil.

Previous studies by Devaprakasam et al. (15), Khatri and Biswas (16), and by Das et al. (17) have all shown that the structure adopted by lubrication additives plays a major role in the antiwear performance in steel on aluminum contact scenarios. The precise orientation and conformational structure adopted by lubrication additives upon adsorption, such

\* Corresponding author. E-mail: mtlc2@cam.ac.uk. Phone: 44 1223 336526. Fax: 44 1223 336362.

Received for review March 24, 2009 and accepted July 9, 2009

DOI: 10.1021/am900199f

© 2009 American Chemical Society

as oleamide is therefore key to understanding their lubricating action (18, 19). This study therefore seeks to determine the conformational ordering and polar orientation of an in situ oleamide film adsorbed on an aluminum surface from low concentrations of oleamide in oil. This requires the use of interface techniques that are sensitive to molecularly thick films. In the present study, two complementary surface vibrational spectroscopy techniques are used; the non linear optical technique of sum frequency generation (SFG) spectroscopy and reflection absorption infrared spectroscopy (RAIRS). The RAIRS technique has been successfully used in the past to study thin hydrocarbon films on metals such as gold and aluminum under air using *p*-polarized infrared light, which produces infrared spectra of functional groups having their transition dipoles parallel to the surface normal. Additionally, it provides a qualitative measure of the concentration of the molecules at or in proximity to the surface having this net orientation. RAIRS has proven particularly useful for determining the tilt angles of aliphatic chains relative to the surface normal. SFG spectra provide complementary data to RAIRS. In particular, SFG is interface-specific and possesses submonolayer sensitivity. It is therefore an appropriate technique to detect the formation of molecular films forming from solution under equilibrium conditions, e.g., oleamide adsorbing from oil, without interference from the bulk solution overlayer, a use for which RAIRS is inappropriate because of the excessive signal obtained from the bulk superphase.

The main structural data provided by SFG relevant to the present study is (i) the absolute orientation of functional groups of molecules adsorbed on metal surfaces and (ii) the conformational order in the surface film. The majority of the work reported so far is on oleamide films under air, both spin-cast and L–B deposited. These have quite different thicknesses and structures from each other and as stated earlier can be considered to represent the extremes of order/disorder that might be expected to arise in a hydrocarbon-based film on a metal surface. To understand the structure of films under oil measured by SFG we first examined films with a well characterized structure (low and high compression L–B films) under air using both SFG and RAIRS. These spectra were then taken as a benchmark for the structure of the film observed under oil in the SFG spectra. Specifically we have compared the SFG spectra of low compression (1 mN m<sup>-1</sup>) and high compression (25 mN m<sup>-1</sup>) L–B and spin-cast films recorded in air, where their structure has been well characterized by SFG, RAIRS, and ellipsometry, with their structure under oil. The spectra under oil were in turn compared with oleamide films formed by equilibrium adsorption from oil. Finally, the temporal stability of the preformed films under oil were studied over periods of several days using SFG. This has led to the conclusion, based on the SFG results, that the structure of these films after several days in contact with oil are closely similar to the films formed by equilibrium adsorption from a solution of oleamide in oil.

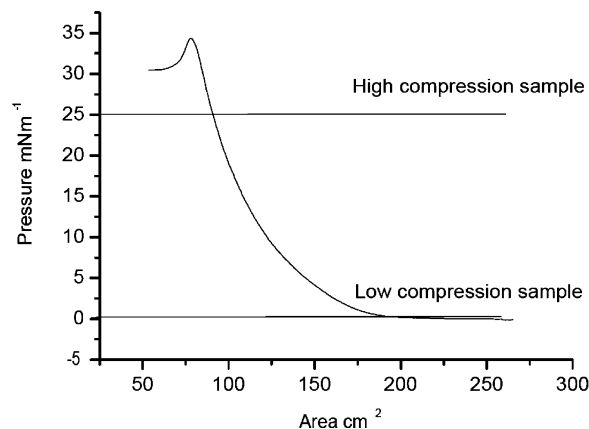
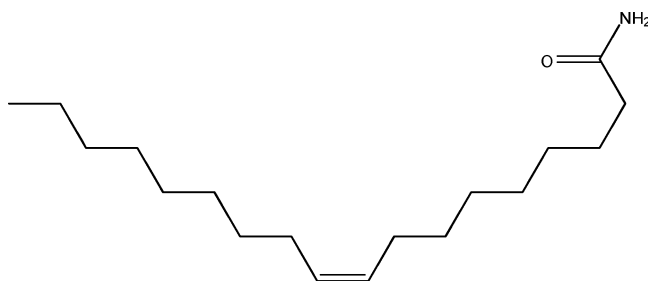


FIGURE 1. Surface pressure/area isotherm for oleamide cast from chloroform onto a water subphase. The pressures at which the 1 and 25 mN m<sup>-1</sup> L–B films were drawn are indicated.

## EXPERIMENTAL SECTION

Aluminum substrates were prepared on silicon wafers by thermal evaporation and a random selection of the substrates imaged by scanning electron microscopy in order to estimate the thickness of the metal film. Average film thicknesses of 200 nm were found. Samples for SFG examination were 1 cm<sup>2</sup> in size in order to fit into the liquid cell of the SFG experiment. Spin-cast films were produced by spin coating at 2000 rpm for 10 min (Laurell Technologies WS-400B-6NPP/lite spin coater). HPLC grade methanol was used as the solvent for spin-cast films. The L–B films were prepared on 75 mm × 15 mm aluminum coated silicon samples, which presented a sufficiently large surface area to obtain RAIRS spectra. Samples were immersed in a subphase of Millipore 18.2 MΩ cm<sup>-1</sup> water in an L–B trough (Nima 611) prior to casting of oleamide from an HPLC grade chloroform solution onto the water surface. The chloroform was allowed to evaporate until a stable surface pressure was achieved (minimum 45 min). A surface pressure isotherm was recorded prior to deposition; a representative isotherm is shown in Figure 1. The oleamide film was then compressed and held at a constant surface pressure of either 1 or 25 mN m<sup>-1</sup> and the aluminum sample withdrawn through the film-air interface at a rate of 5 mm min<sup>-1</sup>. The resulting films were then dried under a nitrogen stream for 10 min. Ellipsometric thicknesses were recorded at an incident angle of 70° using a single-frequency (632.8 nm) ellipsometer; 12 points per sample were recorded and averaged for the final result.

Oleamide (99%) (structure shown below) from Aldrich and per-deuterated hexadecane from QMX laboratories were used as received. All glassware, o-rings, and stainless steel components were cleaned following standard procedures (20, 21) and rinsed 20 times with 18.2 MΩ cm<sup>-1</sup> Milli-Q water and dried under a nitrogen stream before use. Aluminum samples were rinsed in hplc grade methanol upon removal from the evaporator chamber and then rinsed in ultrapure (Millipore 18.2 MΩ cm<sup>-1</sup>) water before storage in sealed glass vials under ultrapure water until used.



RAIRS spectra of the films in air were recorded on a Perkin-Elmer Spectrum 100 FTIR spectrometer equipped with a liquid nitrogen cooled mercury cadmium telluride (MCT) detector covering the range 400–4000  $\text{cm}^{-1}$ . 512 scans at a resolution of 4  $\text{cm}^{-1}$  were coadded to achieve the final spectrum. All spectra were recorded at least 3 times on an individual sample and a minimum of 3 samples were used at each surface pressure. The RAIRS spectra of films under oil were found to vary considerably and are therefore not included here. This was due to the varying thickness of deuterated oil on the sample surface, and the presence of a significant C–D overtone band in the N–H stretching region and a single strong peak in the C–H stretching region that dominated any spectra.

SFG (22) spectra were recorded on a nanosecond spectrometer (10 ns pulse duration at a repetition rate of 11.5 Hz), details of which can be found elsewhere (23, 24), in both PPP and SSP polarization combinations (sum frequency, visible, infrared) in a counter propagating beam geometry. The samples under oil were examined in a stainless steel cell with an integral calcium fluoride prism. Samples were mounted on a vacuum chuck held on a three axis micrometer-controlled mount. Samples were immersed in oil or oil–oleamide for 30 min prior to advancing the sample under micrometer control to less than 1  $\mu\text{m}$  from the prism surface. The sample was then retained at the prism surface under non flowing conditions for the duration of the spectral acquisition. The input beams of the IR and visible lasers were set at angles of 60 and 65° respectively to the surface normal at the metal–oil or metal–air interface. Separation of the SFG output from reflected 532 nm radiation was achieved through a 532 nm holographic notch filter and a combination of edge and band-pass filters. Sixty shots per point were coadded on a digital storage oscilloscope (Le Croy) at 2.1 Giga samples per second and the spectra were scanned at intervals of 2  $\text{cm}^{-1}$  between 2800 and 3400  $\text{cm}^{-1}$ . Multiple spectra were then coadded until the signal-to-noise ratio was deemed acceptable. No SFG spectra were detected in the N–H stretching region, and therefore results are only presented for the 2800–3000  $\text{cm}^{-1}$  range. Individual spectra were coadded for up to 6 h and normalized to an aluminum reference surface recorded either in air or under oil as appropriate before analysis. Repeat spectra of at least three samples were recorded to ensure the reproducibility of the results.

For a metal surface, only polarization combinations that contain P polarized IR give rise to significant SFG intensity due to the metal surface selection rule and the high reflectivity of metal surfaces in the IR region. Therefore, for aluminum surfaces, only the SSP and the PPP polarization combinations are relevant. In the SSP polarization combination, only modes that have transition dipole moments with a component perpendicular to the surface appear in the observed SFG spectra, as only a single component of the nonlinear susceptibility  $\chi^{(2)}_{yyz}$  is probed in this combination (where the subscript refers to the orientational alignment of the sum frequency signal, visible pump, and IR pump beams, respectively). As the IR component resides solely in the  $z$  axis, only transition dipoles with a component in this orientation will be probed. On the other hand, spectra in the PPP combination contain contributions from several susceptibility components, specifically  $\chi^{(2)}_{zzz}$ ,  $\chi^{(2)}_{xxx}$ ,  $\chi^{(2)}_{xzx}$ , and  $\chi^{(2)}_{zxx}$ . IR-active vibrations in both the  $z$  and the  $x$  axes are therefore capable of giving rise to an SFG signal in the PPP beam polarization, i.e., this polarization probes vibrational resonances with transition dipole moments oriented both parallel and perpendicular to the surface.

As sum frequency generation is forbidden in systems that possess a center of inversion symmetry SFG spectra arise solely from the interface where bulk phase inversion symmetry is broken, i.e., there is no spectral contribution from the overlying bulk medium. Additionally, no SFG signal can arise from a surface film that is entirely randomized or from a specific

vibrational mode that is locally centrosymmetric, such as the  $\text{CH}_2$  moiety in an all trans aliphatic hydrocarbon chain. A complete theoretical description of the theory of SFG and the various polarization combinations and surface selection rules may be found elsewhere (25).

The modeling of the SFG spectra used a Levenberg–Marquardt least-squares algorithm (26) to fit the resonances to a Lorentzian line profile of the second order susceptibilities. The modeling allows the frequency, strength, and widths of the vibrational resonances to be determined as well as the strength and phase of the nonresonance susceptibilities. The intensity of the recorded signal,  $I_{\text{SF}}$ , depends on both resonance,  $\chi_{\text{R}}^{(2)}$ , and non-resonance,  $\chi_{\text{NR}}^{(2)}$ , susceptibilities

$$I_{\text{SF}} \propto |\chi_{\text{R}}^{(2)} + \chi_{\text{NR}}^{(2)}|^2$$

This equation can then be expanded into polar coordinates

$$I_{\text{SF}} \propto ||\chi_{\text{R}}^{(2)}|e^{i\delta} + |\chi_{\text{NR}}^{(2)}|e^{i\epsilon}|^2 \\ \propto |\chi_{\text{R}}^{(2)}|^2 + |\chi_{\text{NR}}^{(2)}|^2 + 2|\chi_{\text{R}}^{(2)}||\chi_{\text{NR}}^{(2)}| \cos[\epsilon - \delta]$$

where  $\delta$  and  $\epsilon$  are the phases of the resonance and nonresonance terms, respectively. The  $\chi_{\text{R}}^{(2)}$  term itself is given by

$$\chi_{\text{R}}^{(2)} = \frac{B}{(\omega_{\text{v}} - \omega_{\text{IR}} - i\Gamma)}$$

where  $B$  is the strength of the resonance,  $\Gamma^{-1}$  the relaxation time of the vibrationally excited state,  $\omega_{\text{IR}}$  the wavenumber of the IR laser beam, and  $\omega_{\text{v}}$  the wavenumber of a SF active vibration. This equation rearranges to

$$|\chi_{\text{R}}^{(2)}| = \sqrt{\frac{B}{(\omega_{\text{v}} - \omega_{\text{IR}} - i\Gamma)} \frac{B}{(\omega_{\text{v}} - \omega_{\text{IR}} + i\Gamma)}} \\ = \sqrt{\frac{B^2}{(\omega_{\text{v}} - \omega_{\text{IR}})^2 + \Gamma^2}}$$

which has the form of a Lorentzian line shape

$$y = \frac{HW^2}{(\omega_{\text{v}} - \omega_{\text{IR}})^2 + W^2}$$

and hence

$$|\chi_{\text{R}}^{(2)}| = \sqrt{\frac{HW^2}{(\omega_{\text{v}} - \omega_{\text{IR}})^2 + W^2}}$$

with  $B = W\sqrt{H}$ ,  $\Gamma = W$ . Substituting in the Lorentzian parameters for the magnitude and phase of the second-order susceptibility yields

$$I_{\text{SF}} \propto \frac{HW^2}{(\omega_v - \omega_{\text{IR}})^2 + W^2} + |\chi_{\text{NR}}^{(2)}|^2 + 2\sqrt{\frac{HW^2}{(\omega_v - \omega_{\text{IR}})^2 + W^2}} |\chi_{\text{NR}}^{(2)}| \cos\left[\varepsilon - \arctan\left(\frac{-W}{\omega_v - \omega_{\text{IR}}}\right)\right]$$

The least-squares fitting routine uses this equation to simulate the observed spectrum, changing the parameters  $H$ ,  $W$ ,  $\omega_v$ ,  $|\chi_{\text{NR}}^{(2)}|^2$ , and  $\varepsilon$  to minimize the error between the simulation and the experiment. The fitting program models up to 6 resonances, for 5 of which (the principle C–H modes) the phase is generally constrained to a single variable value on grounds of symmetry, the phase of the sixth resonance can be either fixed or freely variable. The phase and strength of the nonresonance background is independent of the phase of the resonance modes and may be either fixed or variable, depending on the substrate concerned.

## RESULTS AND DISCUSSION

Spectra of the clean aluminum surface were recorded in both PPP and SSP polarizations in air and under deuterated oil (not shown). No observable resonances were apparent in either set of spectra.

The SFG results presented here are for the C–H stretching region (27, 28) between 2800 and 3000  $\text{cm}^{-1}$ . No SFG resonances in the N–H stretching region between 3100 and 3400  $\text{cm}^{-1}$  were observed, presumably because of the weak Raman intensity of these modes. The principle C–H modes of interest are the methylene group symmetric stretch ( $d^+$ ) at 2849  $\text{cm}^{-1}$ , the methyl symmetric stretch ( $r^+$ ) at 2870  $\text{cm}^{-1}$ , the methylene asymmetric stretch ( $d^-$ ) at 2920  $\text{cm}^{-1}$  and the methyl asymmetric stretch ( $r^-$ ) at 2953  $\text{cm}^{-1}$ . The Fermi resonances of the methylene ( $d^+_{\text{FR}}$ ) and the methyl symmetric stretching modes ( $r^+_{\text{FR}}$ ) are also present in the SFG spectra and, in contrast to linear infrared, where they are often present only as weak shoulders, may appear as moderately intense bands between 2890 and 2910  $\text{cm}^{-1}$  and around 2932  $\text{cm}^{-1}$  respectively. The C–H olefin stretching band arising from the double bond in the middle of the hydrocarbon chain appears at 3012  $\text{cm}^{-1}$  in the linear infrared spectra, presented later, but is not evident in the SFG results. Also present in the transmission and RAIRS spectra are several bands that can be assigned to the amide headgroup of the oleamide molecule. These comprise the N–H asymmetric and symmetric stretching bands, clearly evident at ca. 3393 and 3358  $\text{cm}^{-1}$  and 3182  $\text{cm}^{-1}$ , respectively. In addition, intense bands, only partly resolved, at 1646 and 1631  $\text{cm}^{-1}$  are assigned to the C=O stretch (amide I) and N–H bend (amide II), respectively.

**(a) Oleamide L–B Films.** Figures 2 and 3 show the SFG spectra of L–B films, formed at pressures of 1 and 25  $\text{mN m}^{-1}$ , deposited on aluminum and recorded in air in both PPP and SSP polarization combinations. The SSP spectrum in Figure 2 top trace shows no evidence of any resonant SFG signals, whereas the PPP spectrum from the same sample shows moderate intensity methylene resonances at 2850

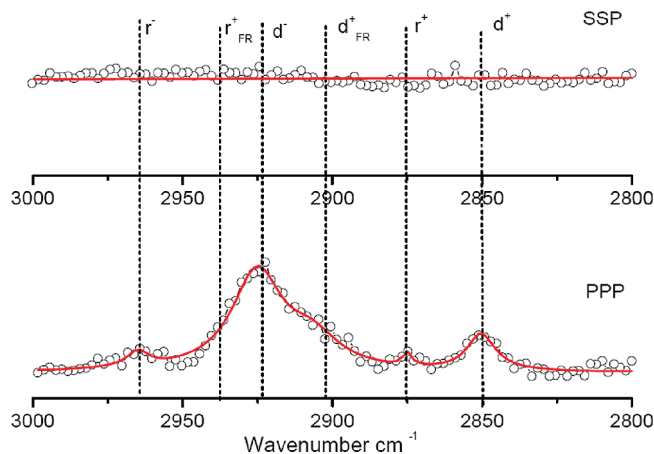


**FIGURE 2.** SSP (top) and PPP (bottom) SFG spectra of an L–B oleamide film deposited on aluminum at a surface pressure of 1  $\text{mN m}^{-1}$ . Spectra recorded in air. Dotted lines show the position of the methyl ( $r$ ) and methylene ( $d$ ) resonances as defined in the text.

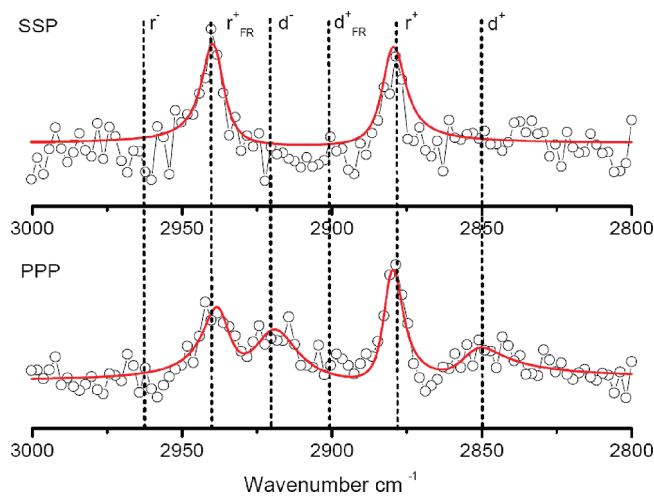


**FIGURE 3.** SSP (top) and PPP (bottom) SFG spectra of 25  $\text{mN m}^{-1}$  L–B film recorded in air.

and 2924  $\text{cm}^{-1}$  and very weak methyl resonances at 2875 and 2963  $\text{cm}^{-1}$ . SFG spectra on metals are generally much weaker in SSP than PPP polarization and the absence of SSP spectra may be due in part to the lower signal:noise ratios achievable with this polarization combination. Nevertheless, the low intensity of the methyl resonances coupled with the much stronger methylene resonances in the PPP spectrum indicates a film in which the hydrocarbon chains have a comparatively low conformational order and an inferred orientation in the plane of the metal/oleamide interface. The ellipsometric thickness of 0.9  $\text{nm} \pm 0.2 \text{ nm}$  determined for the 1  $\text{mN m}^{-1}$  L–B film is compatible with an approximately monolayer thick film.

In contrast, the spectra shown in Figure 3 from the higher pressure L–B film contain resonances in both polarization combinations. In the SSP spectrum there are two intense resonances, from the methyl symmetric stretch at 2878  $\text{cm}^{-1}$  and the methyl symmetric stretch Fermi resonance at 2940  $\text{cm}^{-1}$ . The presence of positive signals relative to the non resonant signal of the aluminum gives an absolute polar orientation for the methyl groups in the adsorbed molecule, namely they are oriented away from the surface. No signifi-

cant methylene mode intensity is observable in the SSP spectrum. The corresponding resonances would be expected to lie at 2850 and 2920  $\text{cm}^{-1}$ . In the PPP spectrum, the methyl symmetric modes are again present; however, there is also a significant contribution to the spectrum from the methylene symmetric mode at 2850  $\text{cm}^{-1}$  and the methylene asymmetric mode at 2920  $\text{cm}^{-1}$ . The methyl asymmetric mode, which usually lies near 2960  $\text{cm}^{-1}$ , is not significantly apparent in the PPP spectrum. Nevertheless, the small feature at 2965  $\text{cm}^{-1}$  may be attributed to this mode but its intensity is too low for spectral modeling to confirm this. No methyl asymmetric mode intensity is apparent in the SSP spectrum.

The dominance of the methyl modes in comparison to the methylene modes in the PPP spectrum and the complete absence of the methylene modes in the SSP spectrum is strong evidence for a well-packed film in which the hydrocarbon chains are oriented along or close to the surface normal. In this situation, there are relatively few gauche defects in the chains and most of the methylene groups are in a locally centrosymmetric environment and therefore SFG inactive. A contribution to the observed methylene resonance intensity in the PPP spectrum may also be due to the presence of the olefin double bond in the oleamide hydrocarbon chain. The two  $\text{CH}_2$  groups adjacent to the unsaturated bond are in a locally noncentrosymmetric environment and can potentially contribute to the methylene SFG signal. As mentioned above, the methyl termination is oriented away from the surface. Support for the proposed structure comes from the ellipsometric film thickness measurement which has a value of  $1.7 \text{ nm} \pm 0.2 \text{ nm}$  consistent with a monolayer film in an extended conformation, i.e., with the film molecules principally oriented normal to the interface.

To gain further insight into the structure adopted by the L–B films, RAIRS spectra of the 1 and 25  $\text{mN m}^{-1}$  L–B films cast on aluminum were compared to a transmission spectrum of bulk oleamide. This spectrum was used as a reference bulk film and shows relative peak intensities consistent with spectra reported in the literature from oleamide in KBr discs, i.e., it is the spectrum from an essentially isotropic orientational distribution. Because of the metal selection rule, RAIRS spectra obtained from a metal surface are sensitive only to modes that have a component of the transition dipole moment in the vertical ( $z$ ) axis (29–31). A comparison of the RAIRS spectra with the transmission spectrum of oleamide with an isotropic distribution therefore allows the degree of orientation of the adsorbed monolayer to be estimated. To compare the L–B spectra with the transmission reference spectrum the latter has been normalized to the methylene asymmetric stretching mode of the L–B spectrum with which it is being compared. Comparison of the C–H region of the 1 and 25  $\text{mN m}^{-1}$  films shows that neither of the RAIRS spectra of the two films exactly matches the relative peak intensities recorded for the bulk oleamide transmission spectrum. Qualitatively the 1  $\text{mN m}^{-1}$  film more closely resembles the transmission spectrum and displays a markedly stronger RAIRS spectrum in absolute

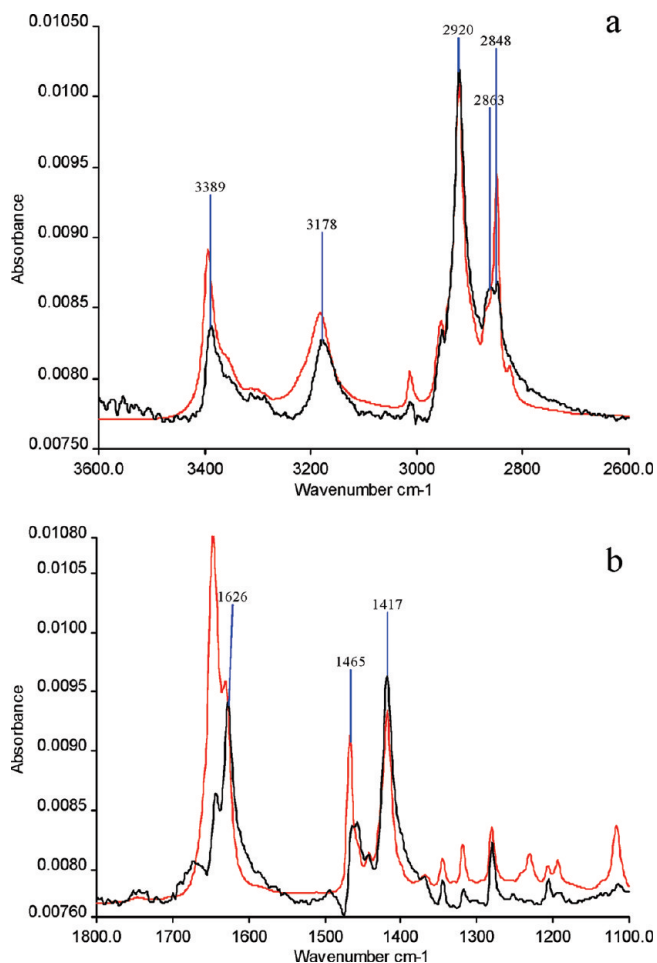
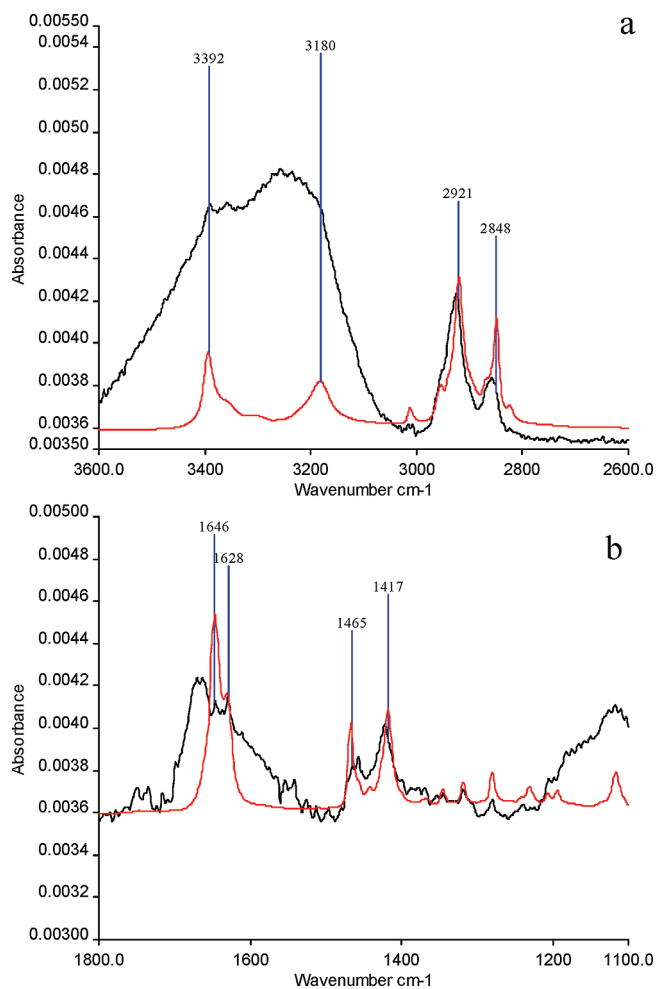


FIGURE 4. Overlay of the 1  $\text{mN m}^{-1}$  L–B film RAIRS spectrum (black) and the bulk transmission spectrum (red) normalized to the antisymmetric methylene mode of the 1  $\text{mN m}^{-1}$  film. (a) C–H stretching region 3600–2600  $\text{cm}^{-1}$ . (b) Amide stretching region 1800–1100  $\text{cm}^{-1}$ .

terms than the 25  $\text{mN m}^{-1}$  film, leading to the general conclusion that both L–B films are less randomly oriented than the transmission spectrum and that the 1  $\text{mN m}^{-1}$  film is more randomly oriented than the 25  $\text{mN m}^{-1}$  film.

The transmission spectrum and the 1  $\text{mN m}^{-1}$  RAIRS spectrum in the C–H and the N–H stretching regions are shown in Figure 4a. Both the methyl and methylene C–H modes are clearly resolved along with the asymmetric and symmetric N–H modes of the amide headgroup which lie at 3393, 3358, and 3182  $\text{cm}^{-1}$ , respectively. The intense bands at 1646 and 1631  $\text{cm}^{-1}$  shown in Figure 4b are assigned to the C=O (amide I) stretch and N–H bend (amide II) mentioned earlier. Comparing the 1  $\text{mN m}^{-1}$  film RAIRS spectrum with the normalized transmission spectrum, two N–H peaks are clearly evident in the RAIRS spectrum but are diminished in intensity in comparison to the  $\text{CH}_2$  asymmetric mode. The C=O amide I band is markedly weaker in the RAIRS spectrum in comparison to the transmission spectrum. The amide II band however shows little reduction in intensity between the two spectra. This indicates stronger ordering of the amide C=O bond in the plane of the interface compared with the bulk film. Furthermore, as a significant component of the intensity of the in-plane bending mode



**FIGURE 5.** Overlay of the 25  $\text{mN m}^{-1}$  L-B film RAIRS spectrum (black) and the bulk transmission spectrum (red) normalized to the antisymmetric methylene mode of the 25  $\text{mN m}^{-1}$  film. (a) C-H stretching region 3600–2600  $\text{cm}^{-1}$ . (b) Amide stretching region 1800–1100  $\text{cm}^{-1}$ .

of the N-H group remains there is little orientational ordering of the amide N-H group in the plane of the interface relative to the ordering implied by the transmission spectrum. The C-H bands are broadly similar in intensity between the transmission spectrum and the RAIRS spectrum with the exception of the methylene symmetric band at 2849  $\text{cm}^{-1}$  which shows a marked decrease in intensity, indicating that the dipole moment of the methylene symmetric stretch must be orienting preferentially in the plane of the interface in the 1  $\text{mN m}^{-1}$  L-B film.

For the 25  $\text{mN m}^{-1}$  film comparison of the transmission and the RAIRS spectra in the regions of the C-H and N-H bands, panels a and b in Figure 5 show significant differences between them in both peak positions and intensities. In the C-H region the broadband in the RAIRS spectrum centered at 2858  $\text{cm}^{-1}$  is assigned to a combination of the methyl symmetric stretch and a residual methylene symmetric stretch. This was confirmed by deconvoluting and fitting this feature into the two component peaks (not shown). The intensity of the symmetric methylene band is greatly reduced in the RAIRS spectrum in comparison to the transmission spectrum. This suggests that the transition

dipole moment (of this mode), and hence the plane of the  $\text{CH}_2$  groups, is oriented more parallel to the surface than they are in the transmission spectrum. On the other hand, the asymmetric methylene band, whereas slightly blue-shifted, is still strongly evident in the RAIRS spectrum. The methyl symmetric stretch is enhanced in the RAIRS spectrum compared to the transmission spectrum, while the methyl asymmetric stretch, is slightly reduced in relative intensity in the RAIRS spectrum (confirmed by deconvoluting the methylene and methyl asymmetric stretches). The implication of the change in methyl mode intensities is that the methyl groups in the 25  $\text{mN m}^{-1}$  film have a greater degree of orientation of their dipole moments along the surface normal than in the 1  $\text{mN m}^{-1}$  film. The regions containing the N-H stretching bands and the amide I and II bands (Figure 5b) are obscured in the RAIRS spectrum by strong water absorptions that remained after the film was dried. The N-H asymmetric stretch can just be discerned superimposed on the water O-H stretching band. There is also a much weaker shoulder from the symmetric N-H stretch. The amide I and II bands can also be identified but are superimposed on the water bending mode and are extremely weak. The overall conclusion therefore is that for the 25  $\text{mN m}^{-1}$  film, the methylene C-H bonds are predominantly oriented parallel to the surface while the terminal methyl group is oriented with a significant component perpendicular to the surface.

Confirmation of a difference in the orientational ordering between the two L-B films themselves can be obtained from a comparison of the absolute spectral intensities of the 25 and 1  $\text{mN m}^{-1}$  films, shown in Figure 6. This reveals that despite the difficulty in carrying out a quantitative analysis of the bands in the 25  $\text{mN m}^{-1}$  film because of water adsorption, the 25  $\text{mN m}^{-1}$  film spectrum is markedly weaker than the 1  $\text{mN m}^{-1}$  film spectrum. The relatively weak intensity of both the C-H and the amide features in the 25  $\text{mN m}^{-1}$  film suggests that the transition dipoles of the relevant vibrations are aligned more parallel to the surface than in the 1  $\text{mN m}^{-1}$  film spectrum. However, it has not been possible to quantify the extent of these differences.

In summary, both the SFG and the RAIRS spectra indicate that in air the oleamide chains in the 1  $\text{mN m}^{-1}$  film exhibit only a low degree of conformational order and are lying predominantly in the plane of the interface, whereas in the 25  $\text{mN m}^{-1}$  film the chains exhibit a high degree of conformational order and are oriented essentially perpendicular to the surface. These results are as expected for L-B films cast from the gaseous and liquid condensed phases, respectively.

**(b) Adsorbed Oleamide Films under Oil.** Figure 7 shows the SFG SSP and PPP spectra of oleamide adsorbed on aluminum from a 0.1% by weight solution in perdeuterated hexadecane. All the aluminum samples were immersed in the oleamide in oil solution for at least 40 min prior to commencing spectral acquisition. No significant differences were observed in the spectra recorded following

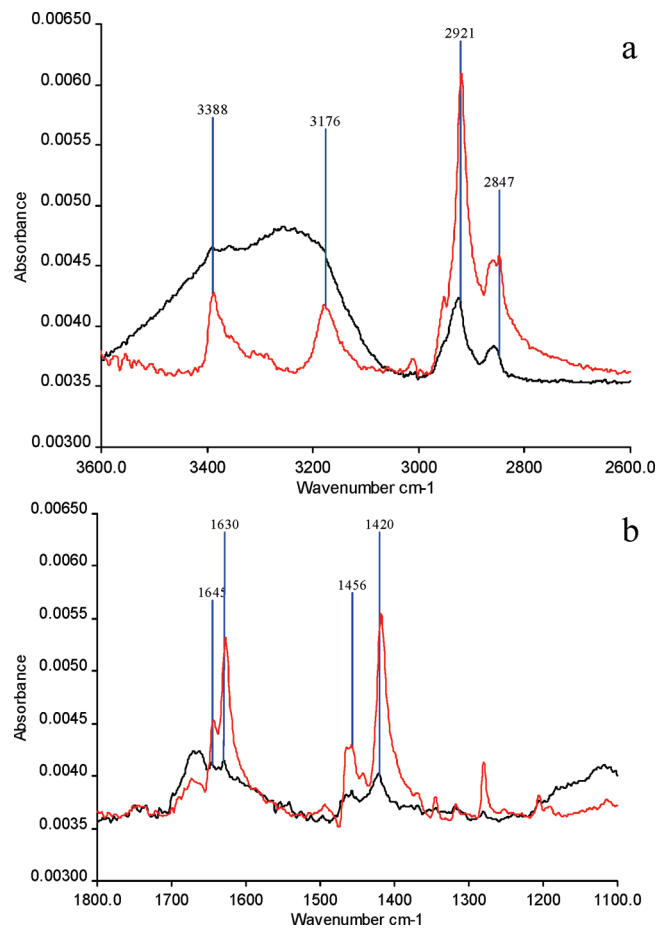


FIGURE 6. Overlay of the  $1 \text{ mN m}^{-1}$  (red) and  $25 \text{ mN m}^{-1}$  (black) RAIRS spectra, both spectra shown to the same scale. (a) C–H stretching region  $3600\text{--}2600 \text{ cm}^{-1}$  (b) Amide stretching region  $1800\text{--}1100 \text{ cm}^{-1}$ .

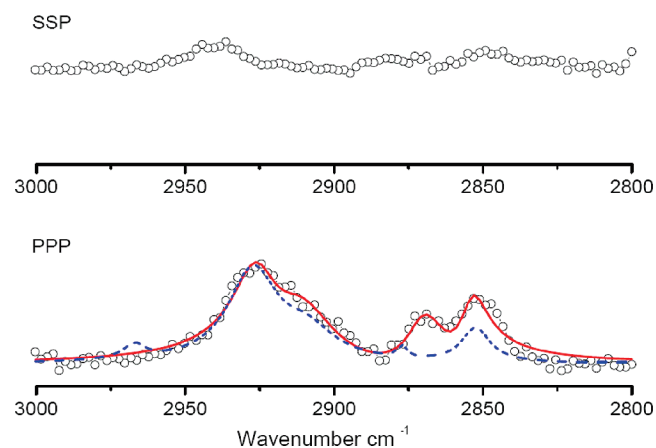


FIGURE 7. SSP (top) and PPP (bottom) SFG spectra of oleamide adsorbed on aluminum from a  $0.1\%$  solution in per deuterated hexane. Blue dashed line is the fit to the  $1 \text{ mN m}^{-1}$  film from Figure 1.

longer immersion times of up to 24 h. The SSP spectrum is extremely weak but a tentative assignment of the features can be given as: the methylene symmetric stretch at  $2850 \text{ cm}^{-1}$ , the methyl symmetric stretch at  $2880 \text{ cm}^{-1}$ , and the methyl symmetric stretch Fermi resonance at  $2940 \text{ cm}^{-1}$ . The observed resonances are, however, too weak to obtain reliable relative intensities from the spectral modeling, and

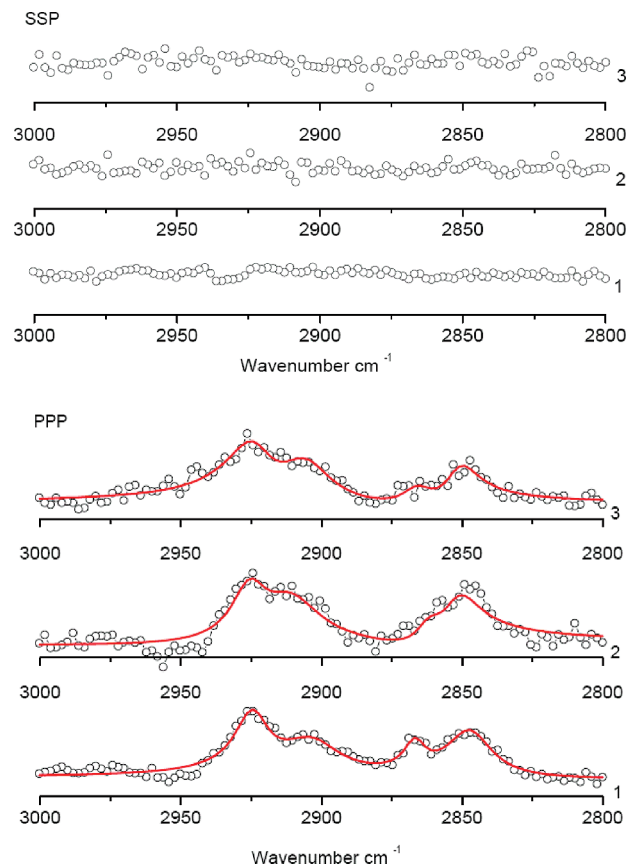
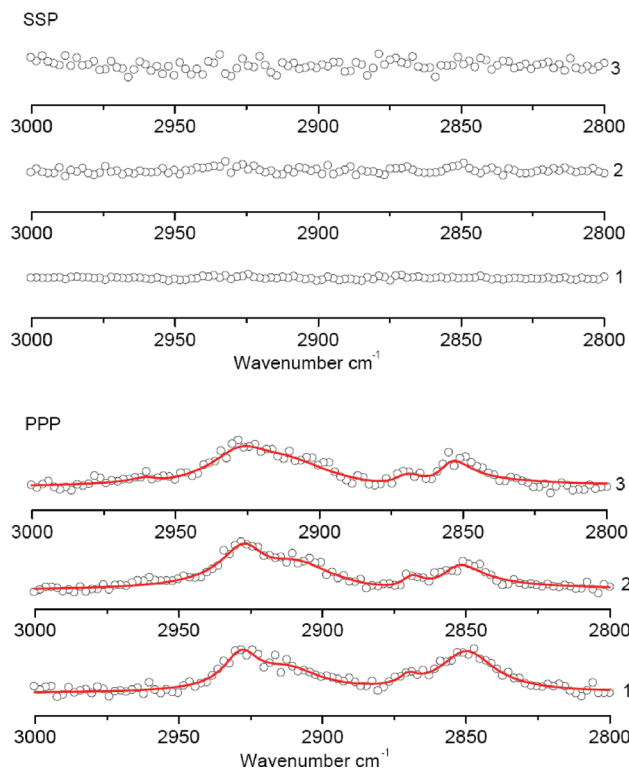


FIGURE 8. SSP (top 3 spectra) and PPP (bottom 3 spectra) SFG spectra of the  $1 \text{ mN m}^{-1}$  film, respectively, as a function of time immersed in per-deuterated oil: (1) as-prepared, (2) 24 h immersion, (3) 48 h immersion.

they are therefore not analyzed in detail. In contrast, the strong PPP spectrum contains well-defined peaks at  $2850$ ,  $2872$ , and  $2925 \text{ cm}^{-1}$  and a weak shoulder at  $2915 \text{ cm}^{-1}$ , all of which can be reliably modeled according to the resonance assignments given previously.

A comparison of the spectra obtained upon adsorption from oil with the spectra of the  $1$  and  $25 \text{ mN m}^{-1}$  L–B films in air shows that, qualitatively, the spectra of the film formed by adsorption from oil is rather more similar to the  $1 \text{ mN m}^{-1}$  film spectra than the  $25 \text{ mN m}^{-1}$  film spectra. Specifically, the significant reduction or absence of an SSP spectrum is apparent in the spectrum adsorbed from oil and in the  $1 \text{ mN m}^{-1}$  L–B spectrum in air, implying that there is little orientational order normal to the surface. Additionally, in both the corresponding PPP spectra, the methylene modes are the dominant features, in marked contrast to the  $25 \text{ mN m}^{-1}$  film spectrum which is characterized by strong methyl resonances. Hence it is reasonable to conclude that the most likely structure for the film adsorbed from oil is that of a relatively disordered monolayer with the oleamide chains lying principally in the plane of the interface.

**(c) Addition of Oil to L–B Oleamide Films.** Figure 8 shows the effect of the addition of oil to both the  $1$  and  $25 \text{ mN m}^{-1}$  films of oleamide as a function of time. Spectrum 1 was recorded after 40 min and spectrum 2 and 3 1 and 2 days later, respectively. For the  $1 \text{ mN m}^{-1}$  film, there are no detectable resonances in any of the spectra as noted for



**FIGURE 9.** SSP (top 3 spectra) and PPP (bottom 3 spectra) SFG spectra of the  $25 \text{ mN m}^{-1}$  film respectively as a function of time immersed in per-deuterated oil: (1) as-prepared, (2) 24 h immersion, (3) 48 h immersion.

the  $1 \text{ mN m}^{-1}$  film in air (Figure 2). The PPP spectra show a slight change in the relative intensities of the observed resonances compared to the same film under air. Specifically, the  $2850$  and  $2875 \text{ cm}^{-1}$  methylene and methyl symmetric resonances in air are significantly stronger under oil relative to the  $2910$  and  $2925 \text{ cm}^{-1}$  resonances, and the  $2875 \text{ cm}^{-1}$  resonance is shifted to  $2865 \text{ cm}^{-1}$ , whereas the  $2955 \text{ cm}^{-1}$  methyl asymmetric resonance is entirely absent under oil. Spectra 2 and 3 change very little as a function of time compared with spectrum 1, with the exception of a minor weakening of the intensity of the methyl symmetric and the methyl symmetric Fermi resonance modes. This observation is taken to indicate that the oleamide film resides in a moderately disordered state oriented predominantly in the plane of the interface, i.e., little structural reordering of the  $1 \text{ mN m}^{-1}$  film occurs on immersion in oil.

For the  $25 \text{ mN m}^{-1}$  film (Figure 9) the spectral changes are far more pronounced upon immersion in oil in comparison to the spectra observed in air. The SSP spectra under oil show no discernible resonant modes, which is in sharp contrast to the two well-defined methyl resonances observed for the same film in air in the SSP polarization. In the PPP polarization all three spectra are significantly weaker under oil than in air and are dominated by strong methylene resonances, in contrast to the methyl resonances that were the prominent features of the spectrum in air. Although the methyl symmetric resonance is apparent in the PPP spectra under oil no significant methyl asymmetric mode is evident for spectrum 1; however, extremely weak methyl asymmetric resonances may be present in spectra 2 and 3 that

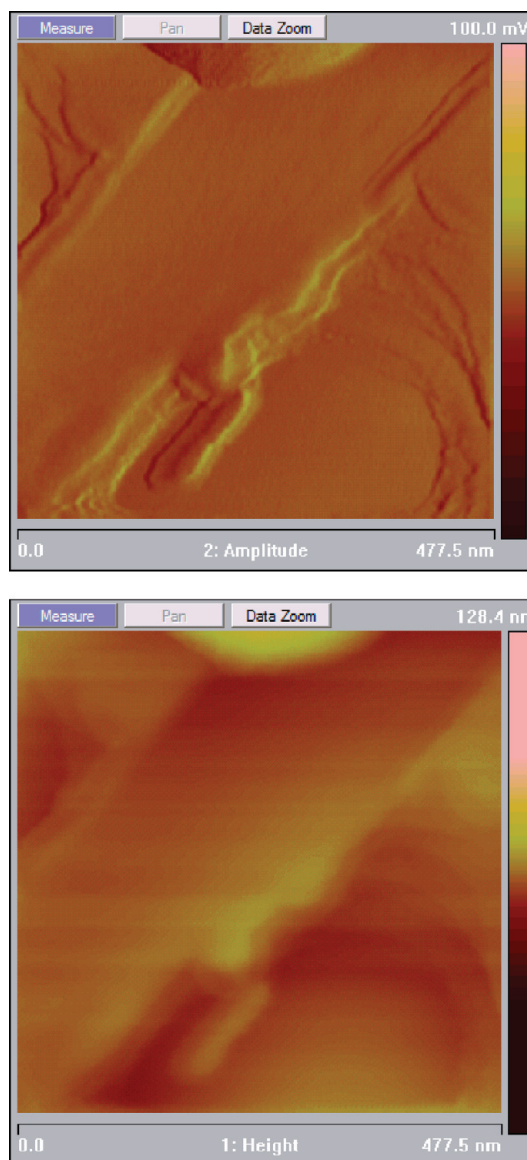


**FIGURE 10.** AFM amplitude and height images of the spin-cast oleamide film in air.

are essentially identical to each other and exhibit only a slight decrease in the relative intensity of the symmetric methyl mode at  $2850 \text{ cm}^{-1}$  relative to spectrum 1.

The spectra recorded for the  $1$  and the  $25 \text{ mN m}^{-1}$  films after immersion in oil for 1 day are essentially identical to each other and show only minor differences when compared to the spectra recorded for the film adsorbed directly from oil (in contrast to the very marked differences between the films recorded in air). It is reasonable to conclude that both L-B films rapidly adopt an equilibrium state similar to that observed upon adsorption from oil within the time frame of the first spectral acquisition (ca. 4–6 h) and that additionally the structure adopted upon immersion in oil appears independent of the initial ordering and surface density of the oleamide monolayer films,

**(d) Thick (Spin Cast) Films in Air and under Oil.** In contrast to the thin L-B films a macroscopically thick, i.e., visible film was also examined. This comprised a spin-cast film with methanol as the casting solvent. This method



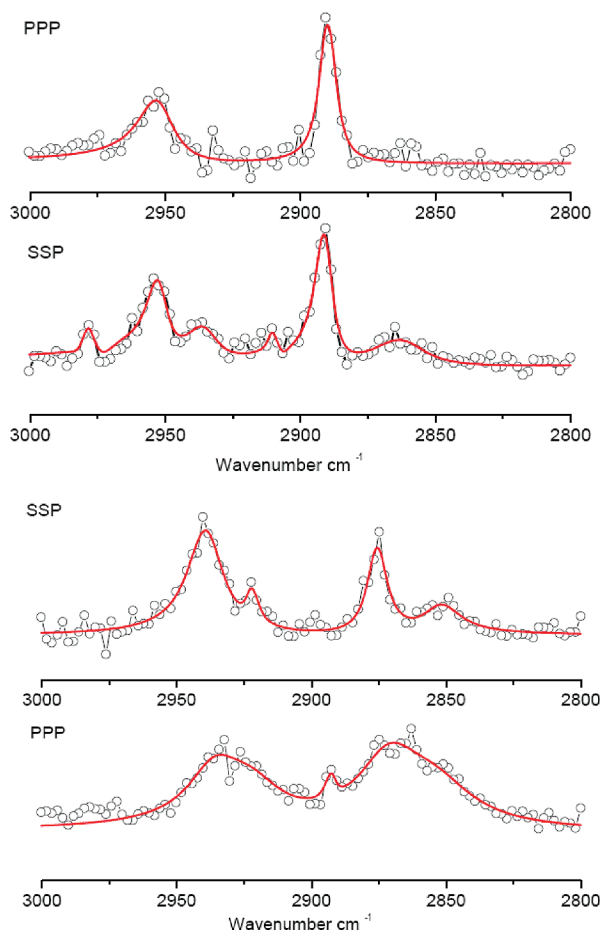


FIGURE 11. SSP and PPP SFG spectra of spin-cast films in air (top 2 spectra) and immediately after immersion in oil (bottom 2 spectra).

produced a film showing a distinct layered structure in the AFM image (Figure 10). The estimated thickness of this film is ca. 0.5–1  $\mu\text{m}$ . The SFG PPP and SSP spectra of the spin-cast film, recorded in air and after immersion in oil, are shown in Figure 11. The PPP spectrum in air shows strong methyl resonances at 2878 (symmetric) and 2940  $\text{cm}^{-1}$  (symmetric FR) with a possible methyl asymmetric resonance at 2968  $\text{cm}^{-1}$  and only weak methylene resonances apparent at 2850, 2890, and 2920  $\text{cm}^{-1}$ , whereas the SSP spectrum in air shows only the methyl 2878 and 2940  $\text{cm}^{-1}$  symmetric resonances indicating a very highly ordered and mostly gauche defect free film, similar to that observed for the 25  $\text{mN m}^{-1}$  film in air.

The SSP spectrum recorded immediately after immersion shows strong methyl resonances at 2978 and 2940  $\text{cm}^{-1}$  and methylene resonances at 2850 and 2920  $\text{cm}^{-1}$ . In broad terms, the SSP spectrum immediately after immersion in oil points to a strong conformational ordering of the amide molecules with a significant degree of polar orientation of the methyl group pointing into the oil phase, which is markedly different to that observed for the 25  $\text{mN m}^{-1}$  L–B film, despite the similar degree of orientation displayed between the two films in air. The PPP spectrum recorded after the SSP spectrum, i.e., ca. 6 h after immersion in oil, however, exhibits a marked broadening of the observed spectral features such that the methyl and methylene reso-

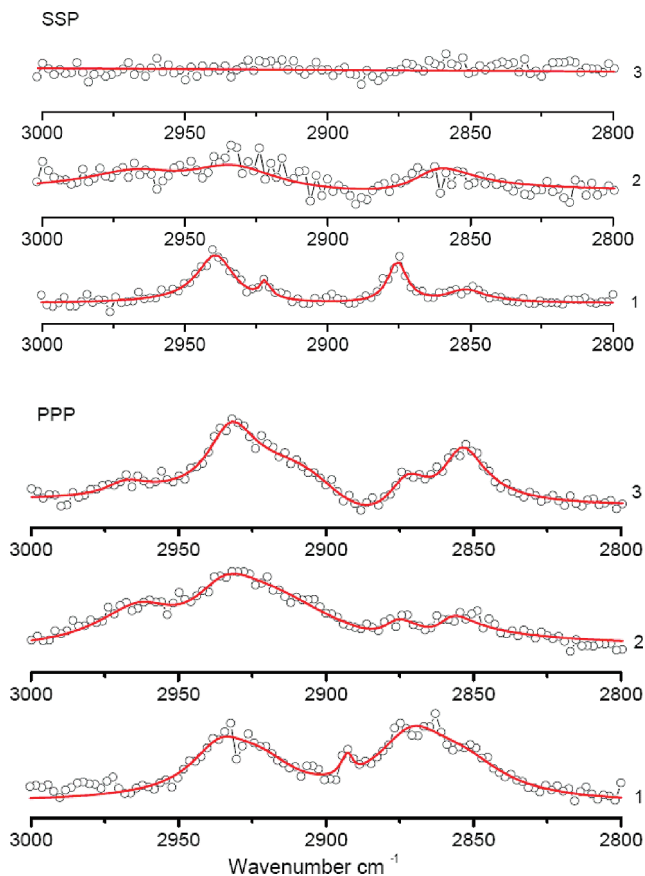


FIGURE 12. SSP and PPP SFG spectra of the spin-cast film as a function of time immersed in oil SSP spectra (top 3 traces), PPP spectra (bottom 3 traces): (1) as-prepared, (2) 24 h immersion, (3) 48 h immersion.

nances cannot be reliably resolved. Modeling of the PPP spectrum shows intensity attributable to both methylene and methyl vibrational resonances indicating a significant decrease in conformational order of the oleamide film on immersion in oil. Several sharp features are apparent in the PPP spectrum that could indicate that methylene groups are present in more than one, i.e., different, conformational environments. It is likely that the initial ordering seen in the SSP spectra is therefore a function of the excess oleamide on the sample surface and the consequent saturation of the overlying oil phase and that the increased conformational disorder seen in the PPP spectrum is due to the additional time that the sample has been immersed in oil prior to the recording of this spectrum. The presence of a strong SSP signal for the spin-cast film demonstrates that the absence of an SSP spectrum in the 25  $\text{mN m}^{-1}$  film is unlikely to be accounted for by the differing Fresnel factors of the oil–film interface in comparison to the air–film interface, as the Fresnel factors for a ca. 1  $\mu\text{m}$  thick oleamide film under oil are similar to those of the 1  $\mu\text{m}$  thick hexadecane superphase used in the experimental cell.

Further spectra recorded at intervals of 1 day are shown in Figure 12. In order to aid comparison spectrum 1 reproduces the spectra recorded immediately after immersion in oil as already discussed. The SSP spectrum of the film after immersion under oil for 24 h (spectrum 2) shows 3 broad and poorly defined resonances at around 2860, 2940, and

2960  $\text{cm}^{-1}$ . After 48 h, no spectral features can be resolved (spectrum 3). The PPP spectrum under oil recorded after immersion for 24 h (spectrum 2) shows at least five spectral resonances, two weak resonances at 2850 and 2875  $\text{cm}^{-1}$  attributed to the methylene and methyl symmetric stretching modes, respectively, and three further resonances at 2910, 2930, and 2960  $\text{cm}^{-1}$  that correspond to the previously assigned methylene modes. After a further 24 h immersion in oil, the PPP spectrum is effectively identical to that seen in the previous figures for the 1 and 25  $\text{mN m}^{-1}$  L–B films recorded under oil.

From these results, it is clear that the surface of the spin-cast oleamide film retains a high degree of conformational ordering and orientational alignment in the  $z$  axis immediately after immersion in oil. As time elapses, however, a gradual disordering occurs, as indicated by the broad features recorded in spectrum 2 in both the PPP and SSP polarizations. The spectra recorded for day 1 and 2 are not reproducible in detail, as they vary according to the time the sample has spent immersed in oil. By the third day, the spectra are highly reproducible and identical to the spectra recorded for the 1 and 25  $\text{mN m}^{-1}$  films recorded under oil. It is reasonable to conclude therefore that the film is now in equilibrium with amide in solution.

## CONCLUSION

Both SFG spectra and RAIRS confirm that the structure of the 25  $\text{mN m}^{-1}$  film in air is typical of that seen for high compression L–B depositions, namely the backbone of the molecule is predominantly perpendicular to the surface and with a high degree of conformational ordering of the hydrocarbon chain. On the other hand the structure adopted by the 1  $\text{mN m}^{-1}$  oleamide L–B film in air is principally disordered with evidence of limited preferential orientation in the plane of the interface. The film of oleamide adsorbed on aluminum from oil appears to possess only moderate conformational ordering of the hydrocarbon chains, with the molecules lying predominantly in the plane of the interface. The low compression 1  $\text{mN m}^{-1}$  L–B film in air most closely resembles that of the film adsorbed from oil in both orientation and conformational ordering and, as for the adsorbed film, appears to orient with a significant component in the plane of the interface. For both the high compression L–B and the spin-cast films under oil, the SFG spectra indicate that there are a considerable number of gauche defects present in the oleamide film after immersion in oil that are absent in the same films in air. The SFG spectra clearly show that the preadsorbed films with the exception of the 1  $\text{mN m}^{-1}$  L–B film undergo a structural rearrangement on immersion in oil, with both the 25  $\text{mN m}^{-1}$  L–B and spin-cast films becoming markedly more conformationally disordered. For all the films, the final equilibrium spectra under oil are remarkably similar to each other and it is concluded

that the equilibrium surface structure of oleamide under oil on an aluminum surface comprises a moderately disordered film lying predominantly along the plane of the interface and with the terminal methyl group polar orientation pointing away from the metal surface.

## REFERENCES AND NOTES

- (1) Akanmu, M. A.; Adeosun, S. O.; Ilesanmi, O. R. *Behav. Brain Res.* **2007**, *182*, 88.
- (2) Hiley, C. R.; Hoi, P. M. *Cardiovasc. Drug Rev.* **2007**, *25*, 46.
- (3) Ohba, Y.; Kanao, Y.; Morita, N.; Fujii, E.; Hohrai, M.; Takatsuji, M.; Hirose, H.; Miura, D.; Watari, A.; Yutsudo, M.; Zhao, H.; Yabuta, N.; Ito, A.; Kita, Y.; Nojima, H. *Int. J. Cancer* **2007**, *121*, 47.
- (4) Solomonia, R.; Nozadze, M.; Mikautadze, E.; Kuchiashvili, N.; Kiguradze, T.; Abkhazava, D.; Pkhakadze, V.; Mamulaishvili, I.; Mikeladze, E.; Avaliani, N. *Bull. Exp. Biol. Med.* **2008**, *145*, 225.
- (5) Briscoe, B. J.; Tabor, D.; Mustafae, V. *Wear* **1972**, *19*, 399.
- (6) Sharma, A. H.; Beard, B. C. *J. Vinyl Addit. Technol.* **1997**, *3*, 309.
- (7) Huang, W.; Hou, B.; Liu, M.; Li, Z. *Tribol. Lett.* **2005**, *18*, 445.
- (8) Huang, W. J.; Du, C. H.; Li, Z. F.; Liu, M.; Liu, W. M. *Wear* **2006**, *260*, 140.
- (9) Allan, D.; Briscoe, B. J.; Tabor, D. *Wear* **1973**, *25*, 393.
- (10) Fang, J. H.; Chen, B. S.; Liu, W. M.; Dong, L.; Wang, J. Effect of amide type modified rapeseed oil as lubricating additive on friction and wear behavior of steel-steel and steel-aluminum alloy systems. Proceedings of the 4th International Conference on Surface Engineering, Shenzhen, P.R. China, Oct 29–31, 2004; *Transactions of Non-Ferrous Metals Society of China*; Elsevier: New York, 2004; Vol. 14, pp 435–458.
- (11) Rajesh, J. J.; Bijwe, J.; Tewari, U. S. *Wear* **2002**, *252*, PII S0043.
- (12) Gu, Y. J.; Shi, Z. M.; Nie, C. S. *Appl. Spectrosc.* **1998**, *52*, 855.
- (13) Miyashita, N.; Möhwald, H.; Kurth, D. G. *Chem. Mater.* **2007**, *19*, 4259.
- (14) Zhang, R. J.; Möhwald, H.; Kurth, D. G. *Langmuir* **2009**, *25*, 2290.
- (15) Devaprakasam, D.; Khatri, O. P.; Shankar, N.; Biswas, S. K. *Tribol. Int.* **2005**, *38*, 1022.
- (16) Khatri, O. P.; Bain, C. D.; Biswas, S. K. *J. Phys. Chem. B* **2005**, *109*, 23405.
- (17) Das, S.; Varalakshmi, K.; Jayaram, V.; Biswas, S. K. *J. Tribol., Trans. ASME* **2007**, *129*, 942.
- (18) Perry, S. S.; Lee, S.; Shon, Y. S.; Colorado, R.; Lee, T. R. *Tribol. Lett.* **2001**, *10*, 81.
- (19) Harrison, J. A.; Perry, S. S. *MRS Bull.* **1998**, *23*, 27.
- (20) Casford, M. T. L.; Davies, P. B. *J. Phys. Chem. B* **2008**, *112*, 2616.
- (21) Casford, M. T. L.; Davies, P. B.; Neivandt, D. J. *Langmuir* **2006**, *22*, 3105.
- (22) Shen, Y. R. *Nature* **1989**, *337*, 519.
- (23) Lambert, A. G.; Neivandt, D. J.; Briggs, A. M.; Usadi, E. W.; Davies, P. B. *J. Phys. Chem. B* **2002**, *106*, 10693.
- (24) Casford, M. T. L.; Davies, P. B.; Neivandt, D. J. *Langmuir* **2003**, *19*, 7386.
- (25) Lambert, A. G.; Davies, P. B.; Neivandt, D. J. *Appl. Spectrosc. Rev.* **2005**, *40*, 103.
- (26) Lambert, A. G. Resonantly Enhanced Sum Frequency Spectroscopy of Adsorption on Hydrophilic Mica Substrates. Ph.D Thesis, University of Cambridge, Cambridge, U.K., 2001.
- (27) Macphail, R. A.; Strauss, H. L.; Snyder, R. G.; Elliger, C. A. *J. Phys. Chem.* **1984**, *88*, 334.
- (28) Snyder, R. G.; Strauss, H. L.; Elliger, C. A. *J. Phys. Chem.* **1982**, *86*, 5145.
- (29) Francis, S. A.; Ellison, A. H. *J. Opt. Soc. Am.* **1959**, *49*, 131.
- (30) Greenler, R. G. *J. Chem. Phys.* **1969**, *50*, 1963.
- (31) Greenler, R. G.; Snider, D. R.; Witt, D.; Sorbello, R. S. *Surf. Sci.* **1982**, *118*, 415.

AM900199F